Interaction of the antitumour antibiotic luzopeptin with the hexanucleotide duplex d(5'-GCATGC)$_2$

One-dimensional and two-dimensional n.m.r. studies

Mark S. SEARLE,* Jon G. HALL,* William A. DENNY† and Laurence P. G. WAKELIN*‡

*Molecular Pharmacology Group and NMR Facility, Peter MacCallum Cancer Institute, 481 Little Lonsdale Street, Melbourne, Vic. 3000, Australia, and †Cancer Research Laboratory, University of Auckland School of Medicine, Private Bag, Auckland, New Zealand

^{1}H- and ^{31}P-n.m.r. spectroscopy were used to characterize the solution structure of the 1:1 complex formed between the antitumour antibiotic luzopeptin and the self-complementary hexanucleotide d(5'-GCATGC)$_2$. Eighteen nuclear Overhauser effects between antibiotic and nucleotide protons, together with ring-current-induced perturbations to base-pair and quinoline ^{1}H resonances, define the position and orientation of the bound drug molecule. Luzopeptin binds in the minor groove of the DNA with full retention of dyad symmetry, its quinoline chromophores intercalating at the 5'-CpA and 5'-TpG steps and its depsipeptide ring spanning the central two A·T base-pairs. The chromophores stack principally on the adenine base with their carbocyclic rings pointing towards the deoxyribose of the cytosine. There is no evidence for Hoogsteen base-pairing in the complex, all glycosidic bond angles and sugar puckers being typical of B-DNA as found for the free hexanucleotide. The 'breathing' motions of the A·T and internal G·C base-pairs are substantially slowed in the complex compared with the free DNA, and the observation that two phosphate resonances are shifted downfield by at least 0.5 p.p.m. in the ^{31}P-n.m.r. spectrum of the complex suggests pronounced local helix unwinding at the intercalation sites. The data are consistent with a model of the complex in which luzopeptin bisintercalates with its depsipeptide essentially in the conformation found in the crystal of the free antibiotic [Arnold & Clardy (1981) J. Am. Chem. Soc. 103, 1243–1244]. We postulate only one conformational change within the peptide ring, which involves rotation of the pyridazine–glycine amide group linkage by 90° towards the DNA surface. This manoeuvre breaks the glycine-to-glycine transannular hydrogen bonds and enables the glycine NH groups to bond to the thymine O-2 atoms of the sandwiched A·T base-pairs. It also shortens the major axis of the depsipeptide so that the interchromophore distance is more suitable for spanning two base-pairs. The model further implies that the carboxy and hydroxy groups of the L-β-hydroxyvaline residue are appropriately positioned for hydrogen-bonding to the 2-amino group of guanine and the O-2 atom of cytosine of the adjacent G·C base-pair.

INTRODUCTION

Luzopeptin is the principal component of a family of DNA-binding antibiotics that possesses activity against a range of experimental animal tumours [1–4]. Viscometric measurements with closed circular and rodlike DNAs reveal luzopeptin to be a bifunctional intercalating agent [3,4]. It is structurally reminiscent of the bisintercalating antibiotics echinomycin and triostin A [5], being a cyclic depsipeptide substituted with two 3-hydroxy-6-methoxy quinaldic acid chromophores (Fig. 1). X-ray crystallography [5,6] and n.m.r. studies [7] have shown that luzopeptin possesses a two-fold symmetry axis in both crystalline and solution environments. The depsipeptide has a right-handed twisted rectangular β-sheet conformation stabilized by transannular hydrogen bonds between opposing glycine NH and carbonyl groups [5–7]. The major structural features observed in the crystal are also retained in solution, although in the former the chromophores are aligned edge on to one another, rather

than being parallel and orthogonal to the long axis of the depsipeptide as required for bisintercalation [5,6]. Realigning the quinoline groups to produce the staple-like configuration suitable for binding brings the chromophores to within a distance of 1.2–1.45 nm (12–14.5 Å) of each other [5,6], which suggests that luzopeptin has the capacity to span up to three base-pairs when bound to DNA. Footprinting studies indicate that the drug binds best to regions containing alternating A·T base-pairs, although no consensus di- or tri-nucleotide sequence is apparent [8]. The finding that the mobility of DNA complexes of luzopeptin is anomalously retarded on agarose and polyacrylamide gels has led to the suggestion that a proportion of luzopeptin molecules may be bound covalently, forming interduplex cross-links [4,8]. To date there have been no structural studies on luzopeptin–DNA complexes in either the crystalline state or in solution, and consequently geometrical details of the complex remain largely speculative. Specifically, it is not known in which groove of DNA luzopeptin binds, nor

---

Abbreviations used: NOE, nuclear Overhauser effect; NOESY, two-dimensional nuclear-Overhauser-effect spectroscopy; COSY, two-dimensional correlation spectroscopy.
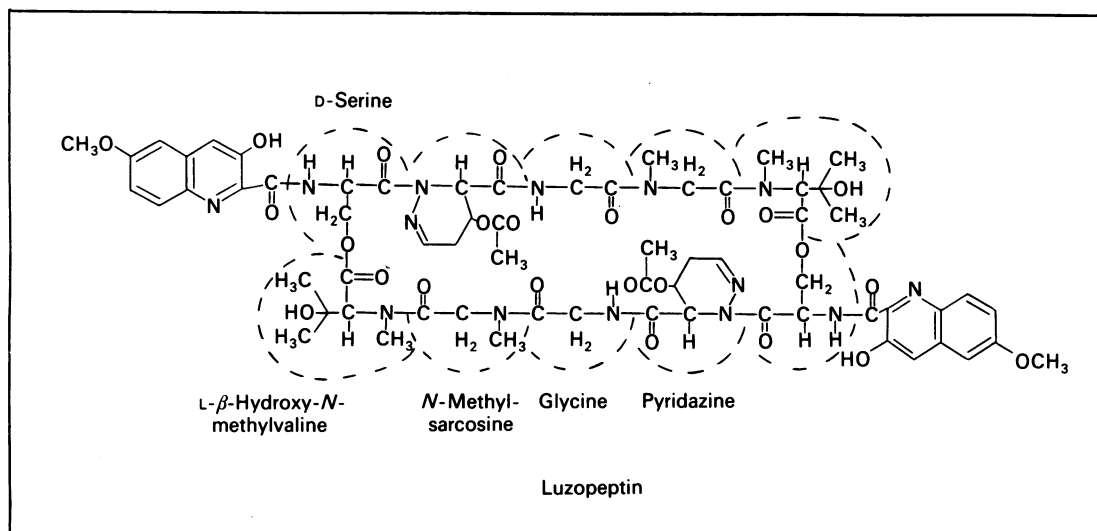   ‡ To whom correspondence should be addressed.

Fig. 1. Structure of luzopeptin

how many base-pairs are sandwiched in the bisinter-calated complex, nor what might be the molecular basis for the sequence selectivity of the binding reaction. Also, given the similarity of the luzopeptin structure to that of the quinoxaline antibiotics, it is of interest to know whether luzopeptin induces radical conformational changes in DNA on binding such as the Hoogsteen base-pairing found in echinomycin–DNA and triostin–DNA complexes [5,9].

Here we describe our initial investigation of the interaction of luzopeptin with the self-complementary hexanucleotide duplex d(GCATGC)$_2$ by the use of two-dimensional n.m.r. spectroscopy. This oligonucleo-tide contains the sequence 5'-CATG, which is a high-affinity binding site for luzopeptin identified in the foot-printing measurements made by Fox et al. [8]. The starting point for any n.m.r. characterization of conformation in small DNA duplexes and their drug complexes involves sequence-specific assignment of resonances in compli-cated ^{1}H-n.m.r. spectra. These assignments are obtained from a combination of two-dimensional n.m.r. experi-ments that identify both scalar coupling interactions (COSY) and through-space dipolar interactions (NOESY). The positions and orientations of bound drug molecules are revealed by intermolecular NOESY con-tacts and by perturbations to the ^{31}P-n.m.r. and ^{1}H-n.m.r. chemical-shift values of the phosphate groups and nucleotide proton resonances. Our preliminary results confirm luzopeptin as a bisintercalating ligand and reveal both the groove disposition of the depsipeptide ring and the sites of intercalative binding. We find no evidence for Hoogsteen base-pairing in the complex, or for any irreversible binding such as alkylation.

MATERIALS AND METHODS

Samples for n.m.r. studies

Luzopeptin was a gift from Bristol Myers and was used without further purification. The hexadeoxyribo-nucleoside pentaphosphate d(5'-GCATGC)$_2$ was pre-pared by a modified version of the phosphotriester method [10]. In the following text the bases are numbered starting from the 5'-end. The aqueous insolubility of

luzopeptin necessitates complex-formation in a mixed organic/aqueous solvent system. Luzopeptin was dis-solved in a small volume of acetone, diluted to 1 ml in methanol/acetone (19:1, v/v) and added to a sample of the oligonucleotide dissolved in 0.5 ml of aq. 50% (v/v) methanol. The solution was further diluted by addition of 3–4 ml of ^{2}H$_2$O and stirred for several hours, then freeze-dried, and the solids were redissolved in 0.6 ml of ^{2}H$_2$O. Excess luzopeptin remained insoluble in ^{2}H$_2$O and was removed by centrifugation. The DNA was not fully complexed in a single step, so the process was repeated four times by redissolving the complexed and unbound DNA mixture in aqueous methanol and adding further quantities of luzopeptin. The extent of complex-forma-tion was monitored at each step by using one-dimensional ^{1}H-n.m.r. spectroscopy. After repeated freeze-drying from ^{2}H$_2$O the sample was dissolved in 0.55 ml of ^{2}H$_2$O containing 10 mM-Na$_2$^{2}HPO$_4$ and 40 mM-NaCl and the pH was adjusted to an uncorrected pH-meter reading of pH 6.9. Considerable losses of DNA were incurred at each step of the above procedure, and the final con-centration of the complexed DNA for n.m.r. studies was approx. 0.5 mM. Also present in the final sample was a small quantity, less than 10%, of uncomplexed d(GCATGC)$_2$, which was in sufficiently low concen-tration so as not to interfere with data collection on the complex. For experiments in ^{1}H$_2$O the sample was freeze-dried and redissolved in ^{1}H$_2$O containing 10% (v/v) ^{2}H$_2$O as a lock signal.

N.m.r. experiments

All ^{1}H-n.m.r. spectra were obtained at 400 MHz on a Varian VXR400/WB spectrometer. Homonuclear ^{1}H double-quantum-filtered COSY and NOESY experi-ments were performed in the phase-sensitive mode with use of the hypercomplex method of data collection [11,12]. Data were acquired with the carrier frequency placed at the centre of the spectrum with quadrature detection in both dimensions: they were recorded as 1024 points in t_2 for each of 320–512 t_1 values. A relaxation delay of 1.5 s was incorporated into each sequence. Datasets were zero-filled to 1024 points in t_1 before Fourier transformation and weighted with an apodiza-

tion function. The final digital resolution was approx. 3.2 Hz/point. ¹H-n.m.r. spectra in solvents comprising ¹H₂O/²H₂O (9:1, v/v) were collected by use of the 1:1 pulse sequence to give on-resonance suppression of the solvent peak [13,14]. One-dimensional NOE difference spectra in ¹H₂O/²H₂O (9:1, v/v) were similarly obtained by using the 1:1 water suppression sequence by subtracting free induction decays obtained in the interleaved mode from on- and off-resonance selective irradiation immediately before acquisition. A selective pre-irradiation period of 300 ms was used with a 1.5 s relaxation delay. ³¹P-n.m.r. spectra were recorded at a frequency of 162 MHz on the VXR400/WB spectrometer with the same 0.6 ml sample used for ¹H-n.m.r. studies. All spectra were obtained with ¹H decoupling using a π/4 excitation pulse with a 1 s relaxation delay. ¹H-n.m.r. chemical shifts are expressed with reference to 3-(trimethylsilyl)-propionic acid at 20 °C, and ³¹P-n.m.r. chemical shifts are referenced to the resonance from the phosphate buffer at pH 7.0. ¹H and ³¹P resonance assignments for d(GCATGC)₂, as well as ¹H assignments for luzopeptin, have been reported previously [7,15,16].

RESULTS AND DISCUSSION

Symmetry of the complex and evidence for bisintercalation

The twofold symmetry of d(GCATGC)₂ and luzopeptin, which results in an equivalence of resonances from the two strands of the duplex and from the two halves of the depsipeptide of the antibiotic [7,15,16], is retained in the complex, as shown by the lack of doubling of resonances in both ¹H-n.m.r. (Fig. 2) and ³¹P-n.m.r.

Fig. 3. 162 MHz ³¹P-n.m.r. spectra of d(GCATGC)₂ and the luzopeptin–d(GCATGC)₂ complex recorded at 20 °C

spectra (Fig. 3). The relative intensity of drug and DNA ¹H resonances indicates a luzopeptin/d(GCATGC)₂ stoichiometry of 1:1 (Fig. 2). This is clearly illustrated by the three methyl singlets of equivalent intensity that appear between 1.0 and 1.5 p.p.m., two of which correspond to the C(γ)H₃ resonances of the β-hydroxyvaline residues and the third to the 5-CH₃ group of the thymine bases. Two of the five phosphate resonances in the ³¹P-n.m.r. spectrum of the complex are shifted downfield by at least 0.5 p.p.m. (Fig. 3) relative to their position in the spectrum of the free hexanucleotide. Such perturbations to the resonances of phosphate groups in the vicinity of the binding site are a ubiquitous consequence of intercalation [16–19], the shifts observed here being very similar to those experienced by two of the three phosphate groups of d(TCGA)₂ in its non-Hoogsteen-base-paired complex with echinomycin [19]. It is also well documented that intercalation induces upfield ring-current shifts on the imino and amino protons of base-pairs adjacent to drug-binding sites [16,17,19]. In the low-field portion of the ¹H-n.m.r. spectrum of the luzopeptin–d(GCATGC)₂ complex in ¹H₂O at 25 °C (Fig. 4) only three imino proton resonances are observed between 11.0 and 13.0 p.p.m., which is again a clear sign of a structure with dyad symmetry. The resonances at 11.59 and 12.63 p.p.m. are assigned to the imino protons of 5-G and 4-T (Table 1) on the basis of the pattern of NOEs observed in the one-dimensional NOE difference spectra shown in Fig. 4 and described below. These resonances have been shifted upfield by 1.02 and 1.20 p.p.m. respectively in the complex (cf. Table I in ref. [16]), which is consistent with intercalation of the chromophores of luzopeptin between the 5'-CpA and 5'-TpG dinucleotide steps.

The above observations lead us to conclude that luzopeptin forms a symmetrical bisintercalation complex with the hexanucleotide in which the central A·T base-
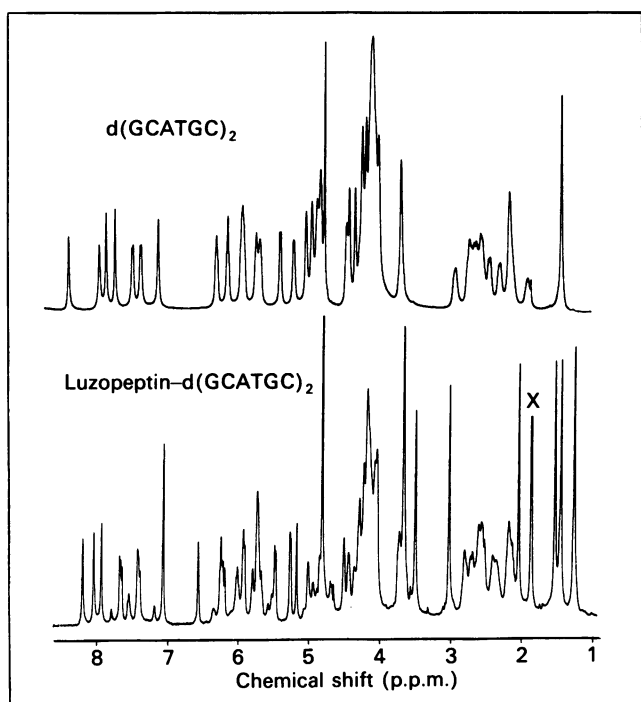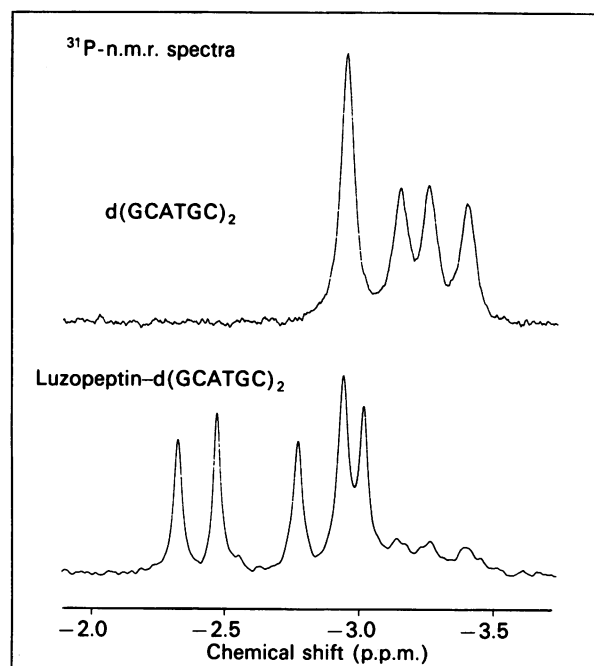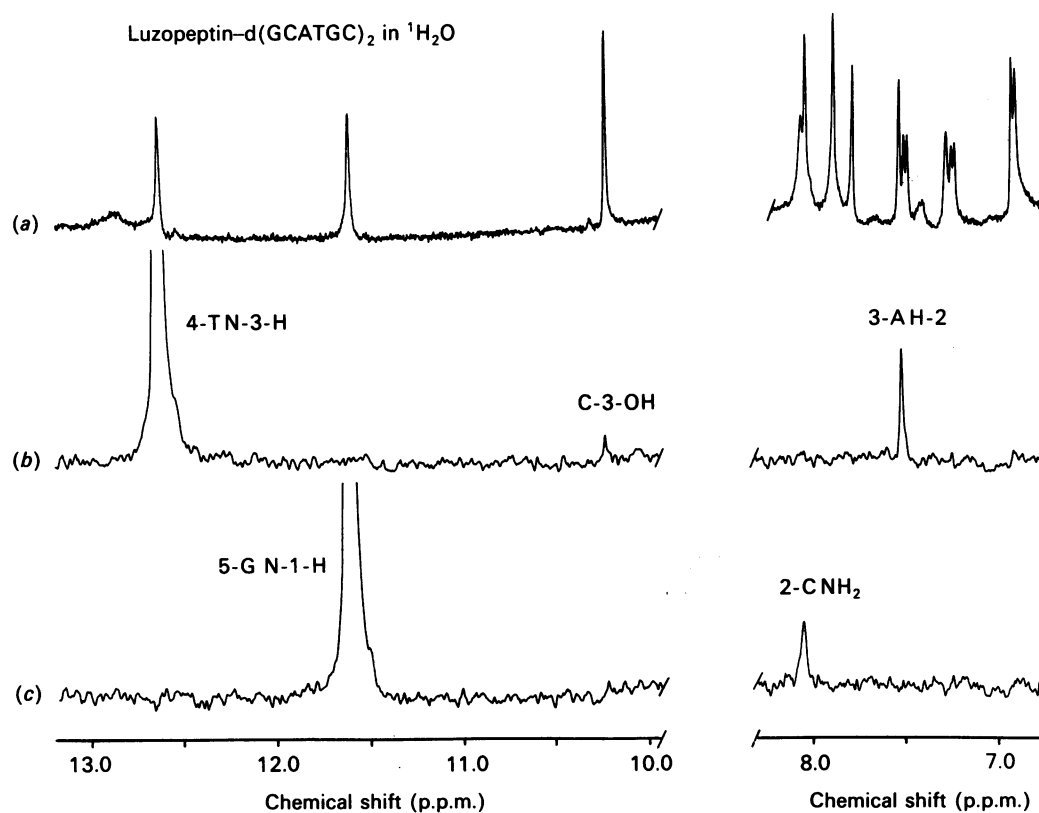

Fig. 2. 400 MHz ¹H-n.m.r. spectra of d(GCATGC)₂ and the luzopeptin–d(GCATGC)₂ complex recorded at 20 °C

X marks the position of a small amount of residual methanol.

Luzopeptin–d(GCATGC)₂ in ¹H₂O

Fig. 4. 400 MHz ¹H-n.m.r. spectrum and NOE difference spectra of the luzopeptin–d(GCATGC)₂ complex recorded at 25 °C in ¹H₂O/²H₂O (9:1, v/v)

Spectrum (*a*) illustrates the aromatic and low-field imino proton resonances; NOE difference spectra observed after 300 ms irradiation of the imino proton resonance of (*b*) 4-T and (*c*) 5-G are also shown.

Table 1. ¹H-n.m.r. chemical shifts of the luzopeptin–d(GCATGC)₂ complex at 20 °C

Abbreviation: N.D., not determined.

	Chemical shifts of the hexanucleotide (p.p.m.)									
Nucleotide	H-1′	H-2′	H-2″	H-3′	H-4′	H-5′/H-5″	H-2	H-5	H-6	H-8
1-G	5.80	2.44	2.62	4.71	4.00	3.34/3.34				7.78
2-C	5.60	2.27	2.32	4.11	N.D.	N.D.		5.14	7.24	
3-A	5.88	2.71	2.71	4.89	4.39	4.04/3.94	7.52			8.04
4-T	5.55	2.12	2.30	4.57	4.02	N.D.		1.37	6.92	
5-G	5.61	2.44	2.52	4.81	4.10	4.05/N.D.				7.89
6-G	6.11	2.06	2.08	4.32	4.15	3.90/4.05		5.35	7.49	

Chemical shifts of luzopeptin (p.p.m.)							
Quinoline H-4	6.92	Serine C_{(α)}H	5.66	Pyridazine C_{(α)}H	5.14	Valine C_{(α)}H	5.05
Quinoline H-5	6.42	Serine C_{(β)}H₂	4.15	Pyridazine C_{(β)}H	5.61	Valine C_{(γ)}H₃	1.18/1.4
Quinoline OCH₃	3.57	Sarcosine C_{(α)}H₂	5.37/4.23	Pyridazine C_{(γ)}H₂	2.51	Valine N-CH₃	3.40
Quinoline H-7	5.78	Sarcosine N-CH₃	2.93	Pyridazine C_{(δ)}H	7.27		
Quinoline H-8	6.02	Glycine C_{(α)}H₂	N.D.	Pyridazine CH₃	1.96		

pairs of the DNA are sandwiched between the drug chromophores. Thus, at least for this sequence, the chromophores of luzopeptin span two base-pairs in a manner analogous to that found for the quinoxaline antibiotics [5,9,19]. A more detailed description of the

luzopeptin–d(GCATGC)₂ complex follows, based on ¹H resonance assignments and NOE-derived distance constraints, in which we are able to define some intermolecular contacts between drug and DNA as well as some conformational characteristics of the complex.
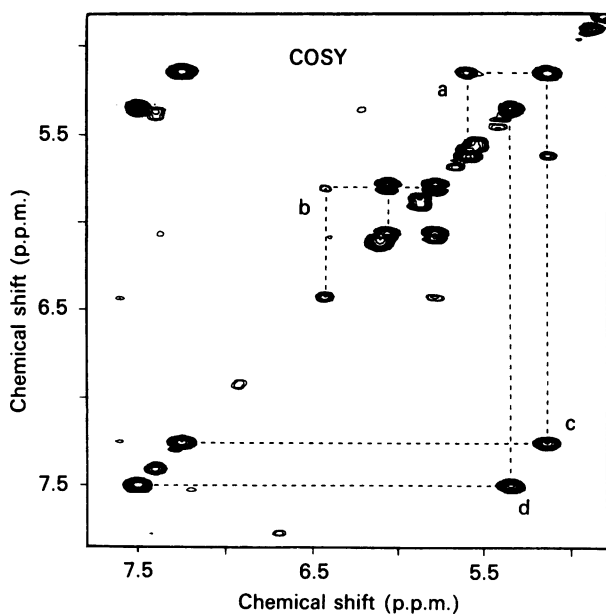
Fig. 5. Portion of the ^{1}H double-quantum-filtered COSY spectrum of the luzopeptin-d(GCATGC)$_2$ complex presented in absolute-value mode

Correlations within the 5.0–7.5 p.p.m. region of the spectrum are illustrated. Identifications: a, pyridazine $C_{(\alpha)}H$ to $C_{(\beta)}H$; b, quinoline H-7 to H-8 and H-7 to H-5; c, 2-C H-5 to H-6; d, 6-C H-5 to H-6.

Assignment of DNA ^{1}H resonances in the complex

The majority of the deoxyribose and all of the base protons in the complex have been assigned from analysis of NOESY and COSY data by using well-established procedures [20–23]. A list of the ^{1}H-n.m.r. chemical shifts identified is given in Table 1. Firstly, scalar coupling interactions were used to identify H-1′, H-2′ and H-2″ within each of the six deoxyribose rings, between H-5 and H-6 of the two cytosine bases (Fig. 5) and between the H-5 and CH$_3$ group of the thymidine. Further correlations within the sugar rings are either weak or not observed. The assignments of H-3′, H-4′ and H-5′/H-5″ were complemented by NOESY data obtained with mixing times of 100 and 250 ms (Fig. 6). To assign resonances to specific residues in the DNA sequence we have used the methodology outlined in refs. [20–23]. The approach exploits the dipolar interactions between the H-6 or H-8 of a particular base and its own sugar H-2′ to make intranucleotide connections, and between H-6 or H-8 and the H-2″ of the nucleotide on the 5′ side of the sequence to assign residues sequentially. This pattern of correlations is of course characteristic of the B-type family of DNA helices to which d(GCATGC)$_2$ belongs [16]. In the NOESY spectrum of the free hexanucleotide (results not shown) the 4-T CH$_3$ group gives an intense cross-peak to the 3-A H-8, establishing both the sequential relationship between 3-A and 4-T and also the right-handedness of the DNA [16,24]. A similar pattern of correlations is observed between these base protons in the complex (Fig. 7), enabling the lowest field resonance to be assigned to the 3-A H-8 as well as verifying the integrity of the base-pair stacking and the right-handedness of the helix in the 5′-ApT core of the drug-
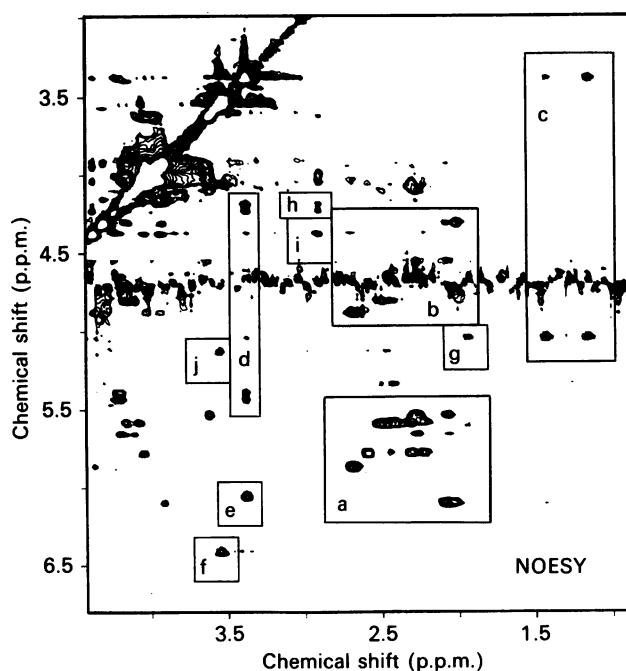

Fig. 6. Portion of the phase-sensitive NOESY spectrum of the luzopeptin-d(GCATGC)$_2$ complex recorded with a mixing time of 250 ms

The following cross-peaks are highlighted: a, nucleotide sugar H-1′ to H-2′/H-2″ plus quinoline H-7 to 2-C H-2′/H-2″ and serine $C_{(\alpha)}H$ to 4-T H-2′/H-2″; b, nucleotide sugar H-2′/H-2″ to H-3′; c, L-N-methyl-β-hydroxyvaline $C_{(\gamma)}H_3$ to $C_{(\alpha)}H$ and $C_{(\gamma)}H_3$ to N-methyl; d, β-hydroxyvaline N-methyl to sarcosine $C_{(\alpha)}H$; e, β-hydroxyvaline N-methyl to quinoline H-8; f, quinoline H-5 to C-6-OCH$_3$; g, L-N-methyl-β-hydroxyvaline $C_{(\alpha)}H$ to pyridazine acetyl methyl; h, sarcosine N-methyl to $C_{(\alpha)}H$; i, sarcosine N-methyl to 3-A H-4′; j, quinoline C-6-OCH$_2$ to 2-C H-5.

bound duplex. Intranucleotide NOEs from the 3-A H-8 and 4-T H-6 to their corresponding H-2′ and H-2″ allow the deoxyribose protons of 3-A and 4-T to be assigned specifically. A sequential NOE from 4-T H-6 to 3-A H-2″ further demonstrates a B-type conformation in the core of the helix. Sequential connections between pyrimidine H-6 and adjacent purine H-2″ are also observed for the 5′-1-Gp2-C and 5′-5-Gp6-C steps in the sequence but not for the purine H-8 to pyrimidine H2′ or H2″ at the 5′-2-Cp3-A and 5′-4-Tp5-G steps (Fig. 7). Disruption of the sequential connections at the 5′-CpA and 5′-TpG dinucleotides provides further evidence that the drug chromophores are intercalated at these sites.

Glycosidic angles and sugar conformations in the complex

Without exception all H-6/H-8-to-H-1′ intranucleotide NOEs in the complex are very weak compared with cross-peaks from H-6/H-8 to H2′ of the same residue or with the cytosine H-5 to H-6 correlations that are observed in the same region of the spectrum (Fig. 8). This pattern of correlations is characteristic of an anti/high-anti configuration about all of the glycosidic bonds in the complex and is the same pattern as found for d(GCATGC)$_2$ alone [16]. More intense intranucleo-
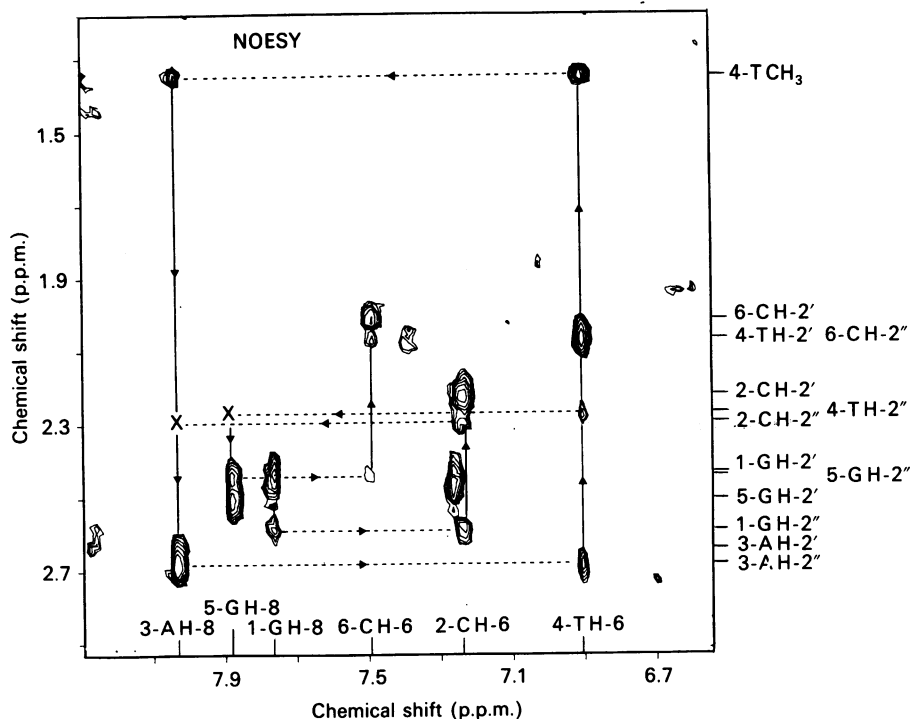
Fig. 7. Portion of the phase-sensitive NOESY spectrum of the luzopeptin–d(GCATGC)$_2$ complex, recorded with a mixing time of 100 ms, identifying correlations between the base proton resonances and sugar H-2′ and H-2″ resonances

Cross-peaks enable sequential assignments to be made in the 5′-direction by identifying H-6/H-8-to-H-2′ intranucleotide NOEs and then H-6/H-8-to-H-2″ internucleotide correlations. X marks the positions where sequential NOEs between 2-C H-2″ and 3-A H-8 and between 4-T H-2″ and 5-G H-8 are expected but not observed, indicating interruption to base-stacking at these points. In the top portion of the Figure a sequential NOE is observed between the 4-T CH$_3$ and 3-A H-8.
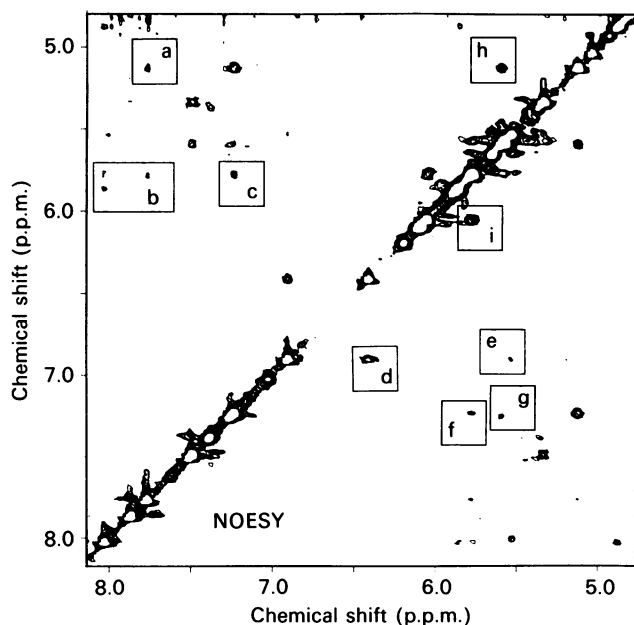

Fig. 8. Portion of the phase-sensitive NOESY spectrum of the luzopeptin–d(GCATGC)$_2$ complex, recorded with a mixing time of 250 ms, illustrating correlations within the 5.0–8.0 p.p.m. region

The following cross-peaks are highlighted: a, 2-C H-5 to 1-G H-8; b, 3-A H-1′ to 3-A H-8, 3-A H-8 to quinoline H-7 and 1-G H-8 to 2-C H-1′; c, 2-C H-6 to quinoline H-7; d, quinoline H-4 to H-5; e, 4-T H-1′ to 4-T H-6; f, quinoline H-7 to 2-C H-6; g, pyridazine C$_{(\delta)}$H to C$_{(\beta)}$H; h, pyridazine C$_{(\alpha)}$H to C$_{(\beta)}$H; i, quinoline H-7 to H-8.

tide NOEs from H-6/H-8 to H2′ than to H-2″, together with very weak H-6/H-8-to-H-3′ correlations, imply that the predominant sugar pucker for all six deoxyribose rings in the complex lies in the C-2′-endo range, again, as observed for d(GCATGC)$_2$ alone [16].

Drug ^{1}H resonance assignments in the complex

The resonances of the quinoline H-7 and H-8 protons of the bound drug are readily identified by the COSY correlation illustrated in Fig. 5, which also shows a long-range coupling between H-7 and H-5 ($\approx$ 1 Hz). An intense NOESY cross-peak from H-5 to a resonance at 6.92 p.p.m. defines the latter signal as originating from H-4. The H-5 resonance also gives a strong cross-peak to a singlet methyl resonance at 3.57 p.p.m., which we ascribe to the C-6-methoxy group. All of the resonances from the chromophores have chemical shifts appreciably upfield of those observed for free luzopeptin (cf. Table 1 with Table 1 in ref. [7]), a finding characteristic of intercalated ligands [16,19]. H-7 and H-8 experience particularly large ring-current-effect contributions of 1.63 and 1.38 p.p.m. to their chemical-shift values, whereas perturbations to the chemical shifts of H-4, H-5 and C-6-OCH$_3$ are smaller but are still greater than 0.4 p.p.m. The two C$_{(\gamma)}$H$_3$ resonances of the β-hydroxyvaline residues are identified between 1.0 and 1.5 p.p.m., and the third of the three methyl resonances in this portion of the spectrum has already been assigned to the 4-T CH$_3$ group. Both valine C$_{(\gamma)}$H$_3$ resonances give strong NOESY cross-peaks to a resolved proton singlet at 5.05 p.p.m., which we ascribe to the β-hydroxyvaline C$_{(\alpha)}$H (Fig. 6).

The $C_{(\gamma)}H_3$ groups and the $C_{(\alpha)}H$ give NOEs to a methyl singlet at 3.40 p.p.m., which we assign to the N-methyl group of the same residue. The methylene protons of the neighbouring sarcosine residue are identified by NOEs to the N-methyl group of the β-hydroxyvaline residue. The highest-field sarcosine $C_{(\alpha)}H$ at 4.23 p.p.m. gives an NOESY cross-peak to the singlet methyl resonance at 2.93 p.p.m., distinguishing the latter as the sarcosine N-methyl group. The remaining unassigned resonance in the aromatic region of the spectrum at 7.27 p.p.m. we ascribe to the $C_{(\delta)}H$ of the tetrahydropyridazine moiety. No COSY correlations are observed from this resonance, but NOESY cross-peaks are identified to protons at approx. 2.5 p.p.m., which we conclude originate from the pyridazine $C_{(\gamma)}H_2$. Correlations between the $C_{(\gamma)}H_2$ and $C_{(\beta)}H$ of this residue are coincident with the H-1′-to-H-2′/H-2″ correlations of the sugar ring of nucleotide 5-G; however, a weak NOESY cross-peak from $C_{(\delta)}H$ to $C_{(\beta)}H$ and strong cross-peaks, both NOESY and COSY, from the $C_{(\beta)}H$ at 5.61 p.p.m. to the pyridazine $C_{(\alpha)}H$ at 5.14 p.p.m. substantiate the assignment of this spin system. The remaining unassigned methoxy resonance at 1.96 p.p.m. we attribute to the acetyl group of the pyridazine residue.

The spin systems of the serine and glycine residues prove to be more difficult to unravel because of overlap with other resonances in the spectrum, and consequently we assign these residues somewhat less confidently. A signal at 5.5 p.p.m. in the region of the spectrum characteristic of sugar H-1′ resonances we attribute to the serine $C_{(\alpha)}H$. This resonance gives NOEs to protons at approx. 4.15 p.p.m., characteristic of serine $C_{(\beta)}H$ protons. The glycine $C_{(\alpha)}H$ protons are expected to appear in the portion of the spectrum containing the resonances of deoxyribose H-4′, H-5′ and H-5″ protons. Poor spectral resolution in this region prevents us from assigning the glycine $C_{(\alpha)}H$ protons unambiguously. All identified bound luzopeptin ^1H-n.m.r. chemical-shift values are included in Table 1.

Intermolecular NOEs and groove binding

NOESY cross-peaks between antibiotic and DNA protons enable us to determine whether luzopeptin is bound in the major or minor groove of the hexanucleotide. The sugar protons H-1′, H-2″ and H-4′ and adenine base proton H-2 all lie in the minor groove of the helix, while the H-5, H-6 and H-8 base protons are located in the major groove. In 250 ms NOESY data we observe cross-peaks between the N-CH₃ group of the L-β-hydroxyvaline residue and 3-A H-2 and 3-A H-4′, and between the sarcosine N-CH₃ group and 3-A H-4′ with a weak effect to 3-A H-1′. We also see cross-peaks from the pyridazine $C_{(\delta)}H$ to 5-G H-4′ and to the resolved 5-G H-5′ proton and from the serine $C_{(\alpha)}H$ to the 4-T deoxyribose H-1′ and H-2′ protons. Some of these NOEs are identified in Figs. 6 and 8. Thus it is clear that the peptide portion of luzopeptin binds in the minor groove of the helix, as illustrated schematically in Fig. 9. The quinoline H-5, H-7 and OCH₃ protons give a set of NOESY cross-peaks to 2-C H-5, 2-C H-6 and 3-A H-8, H7 also being in contact with 2-C H-2′/H2″, showing that the chromophores are intercalated with their substituted edge lying in the major groove. The quinoline–DNA correlations further confirm that the chromophores stack between the 5′-CpA and 5′-TpG steps. A complete list of intermolecular NOESY contacts is given in Table 2.
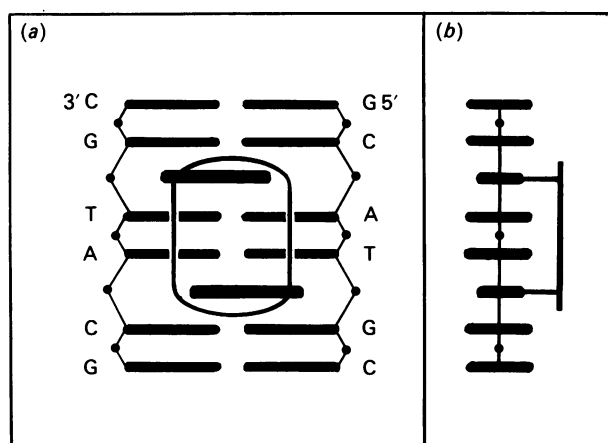

Fig. 9. Schematic representation of the luzopeptin–d(GCATGC)₂ complex with the drug chromophores intercalated at the 5′-TpG and 5′-CpA steps

View (a), depsipeptide ring of luzopeptin lying in the minor groove of the helix. View (b), side-on with the drug chromophores stacked between the base-pairs of the hexanucleotide.

Table 2. Intermolecular NOEs in the luzopeptin–d(GCATGC)₂ complex

Drug proton	DNA proton
Quinoline H-5	2-C H-5
Quinoline OCH₃	2-C H-5, 2-C H-6, 2-C H-3′
Quinoline H-7	2-C H-6, 2-C H-2′, 2-C H-2″, 3-A H-8
Quinoline OH	4-T H-3
Serine $C_{(\alpha)}H$	4-T H-1′, 4-T H-2′, 4-T H-2″
Valine N-CH₃	3-A H-2, 3-A H-4′
Sarcosine N-CH₃	3-A H-1′, 3-A H-4′
Pyridazine $C_{(\delta)}H$	5-G H-5′/H-5″, 5-G H-4′

Conformation of luzopeptin in the complex

The NOESY data provide many intramolecular correlations between adjacent peptide residues that proved useful in assigning the resonances of bound luzopeptin. A number of other correlations reveal interesting conformational features of the bound drug molecule. The orientation of the quinoline methoxy substituent is well defined in the complex, the NOESY data showing the methyl group to be in the plane of the chromophore lying adjacent to the H-5 proton. The quinoline H-8 exhibits a particularly strong NOE to the N-CH₃ group of the L-N-methyl-β-hydroxyvaline residue (Fig. 6), indicating that the chromophores are oriented approximately parallel to the minor axis of the depsipeptide in the complex. Since the ring-current shift and NOESY data are consistent with the notion that the chromophores stack parallel to the base-pairs, it follows that the major axis of the depsipeptide lies approximately at right angles to the plane of the bases. An NOE between the methyl protons of the tetrahydropyridazine residue and $C_{(\alpha)}H$ of L-β-hydroxy-N-methylvaline shows that the acetyl groups stretch across the minor axis of the peptide ring, as found in the free antibiotic [6,7]. Given this, plus the fact that we could detect no intermolecular NOESY contacts

involving the acetyl methyl groups, suggests that in the complex, as observed for free luzopeptin in the crystal [6] and in solution [7], these groups remain disposed on the opposite face of the depsipeptide to the chromophores.

Exchangeable ^{1}H resonances of the complex observed in ^{1}H$_2$O

The ^{1}H-n.m.r. spectrum of the complex in ^{1}H$_2$O at 25 °C reveals four exchangeable proton resonances between 10.0 and 13.0 p.p.m. (Fig. 4). The signals from the imino protons of the internal base-pairs, at 12.63 and 11.59 p.p.m., have narrow line-widths, whereas that of the terminal guanine residue at 12.84 p.p.m. is exchange-broadened. This contrasts with the example of the free hexanucleotide at 25 °C, where the imino proton resonances are exchange-broadened almost to baseline level [16]. The one-dimensional NOE difference spectra of Fig. 4 permit specific assignment of the observed resonances. Irradiating the signal at 12.63 p.p.m. for 300 ms before acquisition results in an intense NOE to 3-A H-2 at 7.48 p.p.m., which identifies the imino proton resonance at 12.63 p.p.m. as that of the 4-T nucleotide. The resonance at 11.59 p.p.m. we thus ascribe to the internal guanine (5-G), which on irradiation exhibits NOEs to the hydrogen-bonded amino protons of 2-C at 8.10 p.p.m. No sequential NOEs are detected between the exchangeable protons of the 5-G and 4-T bases in the complex, confirming that base-pair stacking is disrupted at this point, which is yet more evidence that the drug chromophores are intercalated at the 5'-CpA and 5'-TpG steps. Irradiating the 4-T imino proton results in a small NOE to a resonance at 10.20 p.p.m., which we ascribe to the C-3 hydroxy groups of the intercalated chromophores. We are unable to observe the amide proton resonances of the serine and glycine residues even in spectra recorded at 2 °C.

Overview of the structure and stabilization of the complex

The n.m.r. data paint a picture of a symmetrical luzopeptin–d(GCATGC)$_2$ complex in which the antibiotic intercalates from the minor groove and spans the central two A·T base-pairs, causing only minimal disturbance to the DNA conformation at the nucleotide level. All glycosidic bond angles and sugar puckers in the complex are typical of B-DNA and are as found in the free hexanucleotide [16]. Together with the ^{31}P-n.m.r. data, which show that two phosphate resonances are particularly perturbed in the complex, this suggests that the intercalation cavities arise largely as a result of rotations about the phosphate groups lining the intercalation sites. We find no evidence for Hoogsteen base-pairing or disruption or weakening of the Watson–Crick base-pairs. On the contrary, as may be expected for intercalation complexes, the imino ^{1}H resonances show that the breathing motions of the A·T and internal G·C base-pairs are substantially slowed in the complex compared with the free DNA [16]. Although it appears that luzopeptin may cause irreversible cross-linking in higher-M_r DNA [4,8], we observe no changes to the chemical-shift values of the bases or the phosphate groups indicative of alkylation. Such interactions, if they exist, might of course be sequence-dependent, and our findings do not exclude the possibility of alkylation at other binding sites.

The NOESY spectra and the ring-current-induced modifications to base-pair and quinoline chemical shifts provide several key insights into the geometry of the complex and the forces that contribute to its stability. The experimental data point to a number of strongly stabilizing hydrophobic and van der Waal's interactions. For example, it is clear that the chromophore is intercalated with its carbocyclic ring pointing towards the deoxyribose moiety of the cytosine residues and that it stacks principally, and strongly, on the adenine base. Quinoline–adenine stacking is also a major feature in echinomycin–DNA and triostin A–DNA complexes, although in these cases the adenine is involved in Hoogsteen base-pairing and the stacking pattern must necessarily be different [5,9]. Intermolecular NOEs involving the luzopeptin valine N-methyl group show it to be positioned midway between the adenine H-2 and sugar H-4' protons near the DNA surface, which brings it into close contact with the adenine N-3 and furanose oxygen atoms. By contrast, the lack of intermolecular NOESY contacts to the valine C$_{(\gamma)}$H$_3$ groups suggests that these methyl groups project away from the DNA. Thus the nature of the valine–DNA interaction seems to be similar in luzopeptin–DNA and quinoxaline–DNA complexes [5,9]. The intermolecular NOESY correlations involving the sarcosine N-methyl group reveal this group to be well displaced to the edge of the DNA duplex, adjacent to the adenine sugar moiety. Given its close proximity to the adenine furanose oxygen atom and its lack of contact with the thymine sugar ring, the sarcosine N-methyl group appears to play a different role in the complex from that of the alanine C$_{(\beta)}$H$_3$ groups of echinomycin and triostin A, which wedge between the sugar moieties of the sandwiched base-pairs, causing them to tilt and twist [5,9]. Correlations between DNA and the pyridazine C$_{(\delta)}$H and the serine C$_{(\alpha)}$H show that these protons also make stabilizing van der Waal's interactions with components of the sugar–phosphate backbone.

Taken altogether, the n.m.r. data are consistent with a model for the complex in which luzopeptin binds with its depsipeptide essentially in the conformation found in the crystal of the free antibiotic [6]. Thus it appears that the bound ligand retains its rectangular shape with the valine C$_{(\beta)}$CH$_3$ side chains pointing away from the DNA surface at the 5'-corners of the structure, the 3'-corners being occupied by the serine residues. The side chains of the pyridazine moieties face away from the DNA, stretching across the minor axis of the depsipeptide, and the valine peptide groups lie in the depsipeptide plane with their N-methyl groups pointing towards the DNA backbone. We postulate only one conformational change within the peptide ring, which involves rotation of the pyridazine–glycine amide linkage through 90° in the direction that brings the NH bonds to lie at right-angles to the plane of the depsipeptide on the same face of the molecule as the chromophores. Except for the loss of energy associated with disruption of the transannular hydrogen bonds, CPK (Corey–Pauling–Koltun) molecular models do not reveal any special energetic penalties for this rotation. The main consequences of the manoeuvre are that the major axis of the depsipeptide is shortened so that the interchromophore separation is decreased to a distance suitable for spanning two base-pairs, and that the glycine NH groups are now appropriately positioned for hydrogen-bonding to the thymine O-2 atoms of the sandwiched bases. The latter interaction provides an

explanation for the selectivity of binding across the 5′-ApT dinucleotide and may contribute significantly to the stabilization of the complex. We note that a similar structure can be built spanning the sequence 5′-TpA in which the proposed hydrogen-bonding contacts involve the N-3 atoms of the adenine residues instead of the O-2 atoms of the thymine residues. CPK representations of the model also suggest that the depsipeptide of luzopeptin extends beyond the sandwiched A·T base-pairs, and that the carboxy and hydroxy groups of the L-β-hydroxyvaline residue are appropriately positioned for hydrogen-bonding to the 2-amino group of guanine and the O-2 atom of cytosine of the adjacent G·C base-pair. To form both of these hydrogen bonds simultaneously intercalation must occur on the 3′-side of a cytosine base, which suggests that the sequence-selectivity of luzopeptin may extend to a tetranucleotide binding site. The (postulated) intermolecular hydrogen-bonding potential of luzopeptin is thus maximized at the sequences 5′-CATG and 5′-CTAG.

Since we are unable to resolve the glycine $C_{(\alpha)}H$ and NH resonances in the complex, or those of the 2-amino protons of guanine and the hydroxy proton of the valine residue, we lack direct evidence for the pyridazine–glycine amide linkage rotation and for the proposed hydrogen-bonding schemes. Distance geometry and molecular mechanics calculations will help to refine the structure and provide additional support, or otherwise, for the proposed molecular model.

REFERENCES

1. Ohkuma, H., Sakai, F., Nichigama, Y., Ohbayshi, M., Imariishi, H., Konishi, M., Miyaki, T., Koshiyama, H. & Kawaguchi, H. (1980) J. Antibiot. **33**, 1087–1097
2. Tomita, K., Hoshino, Y., Sasahira, T. & Kawaguchi, H. (1980) J. Antibiot. **33**, 1098–1102
3. Huang, C. H., Mong, S. & Crooke, S. T. (1980) Biochemistry **19**, 5537–5542
4. Huang, C. H., Prestayko, A. W. & Crooke, S. T. (1982) Biochemistry **21**, 2704–2710
5. Wakelin, L. P. G. (1986) Med. Res. Rev. **6**, 275–340
6. Arnold, E. & Clardy, J. (1981) J. Am. Chem. Soc. **103**, 1243–1244
7. Searle, M. S., Hall, J. G. & Wakelin, L. P. G. (1988) Biochem. J. **256**, 271–278
8. Fox, K. R., Davies, H., Adams, G. R., Portugal, J. & Waring, M. J. (1988) Nucleic Acids Res. **16**, 2489–2507
9. Ughetto, G., Wang, A. H.-I., Quigley, G. J., van der Morel, G. A., van Boom, J. H. & Rich, A. (1985) Nucleic Acids Res. **13**, 2305–2323
10. Denny, W. A., Leupin, W. & Kearns, D. R. (1982) Helv. Chem. Acta **65**, 2372–2393
11. Muller, L. & Ernst, R. R. (1979) Mol. Phys. **38**, 963–992
12. Keeler, J. & Neuhaus, D. (1985). J. Magn. Reson. **63**, 454–472
13. Clore, G. M., Kimber, B. J. & Gronenborn, A. M. (1983) J. Magn. Reson. **54**, 170–173
14. Hore, P. J. (1983) J. Magn. Reson. **55**, 283–300
15. Frey, M. H., Leupin, W., Sorenson, O. W., Denny, W. A., Ernst, R. R. & Wuthrich, K. (1985) Biopolymers **24**, 2371–2380
16. Searle, M. S., Hall, J. G., Denny, W. A. & Wakelin, L. P. G. (1988) Biochemistry **27**, 4340–4349
17. Patel, D. J., Kozlowski, S. A., Nordheim, A. & Rich, A. (1982) Proc. Natl. Acad. Sci. U.S.A. **79**, 1413–1417
18. Petersheim, M., Mehdi, S. & Gerlt, J. A. (1984) J. Am. Chem. Soc. **106**, 439–440
19. Gao, X. & Patel, D. J. (1988) Biochemistry **27**, 1744–1751
20. Clore, G. M. & Gronenborn, A. M. (1983) EMBO J. **2**, 2109–2115
21. Hare, D. R., Wemmer, D. E., Chon, S. H., Drobny, G. & Reid, B. (1983) J. Mol. Biol. **171**, 319–336
22. Scheek, R. M., Boelens, R., Russo, N., van Boom, J. H. & Kaptein, R. (1984) Biochemistry **23**, 1371–1376
23. Chazin, W. J., Wuthrich, K., Rance, M., Hyberts, S., Denny, W. A. & Leupin, W. (1986) J. Mol. Biol. **190**, 439–453
24. Patel, D. J., Shapiro, L. & Hare, D. (1986) Biopolymers **25**, 693–706